



Published in final edited form as:

Org Biomol Chem. 2017 April 11; 15(15): 3179–3183. doi:10.1039/c6ob02738e.

Enantioselective Diels-Alder-Lactamization Organocascades Employing a Furan-Based Diene

Mikail E. Abbasov^a, Brandi M. Hudson^b, Weixu Kong^a, Dean J. Tantillo^b, and Daniel Romo^a

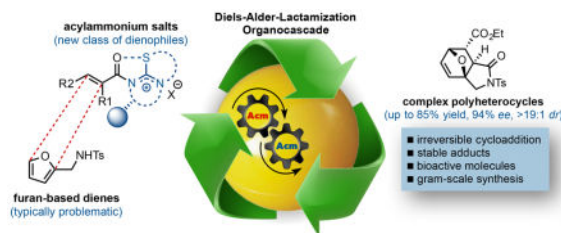
^aDepartment of Chemistry and Biochemistry, Baylor University, One Bear Place 97348, Waco, Texas 76798, United States

^bDepartment of Chemistry, University of California-Davis, One Shields Avenue, Davis, California 95616, United States

Abstract

α,β -Unsaturated acylammonium salts are useful dienophiles enabling highly enantioselective and stereodivergent Diels-Alder-initiated organocascades with furan-based dienes. Complex polycyclic systems can thus be obtained from readily prepared dienes, commodity acid chlorides, and a chiral isothioureia organocatalyst under mild conditions. We describe the use of a furan-based diene bearing pendant sulfonamides leading to the generation of *oxa*-bridged, *trans*-fused tricyclic γ -lactams. This process constitutes the first highly enantio- and diastereoselective, organocatalytic Diels-Alder cycloadditions with these typically problematic dienes due to their reversibility. Computational studies suggest that high diastereoselectivity with these furan dienes may be due to a reversible Diels-Alder cycloaddition for the endo adducts. In addition, the utility of this methodology is demonstrated through a concise approach to a core structure with similarity to the natural product isatisine A and a nonpeptidyl ghrelin-receptor inverse agonist.

Graphical Abstract



A long-standing problem for enantioselective, organocatalytic Diels-Alder (DA) cycloadditions is the use of furan as dienes. Due to their aromaticity, furans are often unreactive and undergo reversible DA cycloadditions, thus strong Lewis acids or high pressure are typically required to promote these cycloadditions.¹ Furthermore, the potential for facile cycloreversion even at lower temperatures,² and the sensitivity to acidic conditions of both the furanyl dienes and cycloadducts typically necessitates immediate post-reaction

Electronic Supplementary Information (ESI) available: Experimental procedures and characterization details for all new compounds including ¹H and ¹³C NMR spectra, computational data, crystallographic data, chiral phase-HPLC traces. Representative examples of unsuccessful DAL reactions employing furan dienes with pendant alcohols.

modification and limit reaction conditions including use of strong Lewis acids. Only two examples of effective catalytic asymmetric DA reactions of furans (67–94% yield, 97–99% *ee*, 4–7.3:1 *endo/exo*) were accomplished by Evans^{3,4} and Corey^{5,6} utilizing chiral bis(oxazoline)Cu(II) and oxazaborolidine Lewis acids **5** and **6**, respectively (Figure 1, **1** → **7**). The former reaction must be conducted at low temperature (−78 °C), due to rapid equilibration at higher temperatures (−20 °C) with concomitant erosion of both *endo/exo* diastereoselectivity and enantioselectivity, while the latter method is limited to the use of 2,2,2-trifluoroethyl acrylate as the only dienophile providing practical yields. Kotsuki attempted the first and only organocatalytic DA reaction of furans catalyzed by 50 mol% *D*-proline under high-pressure (0.8 GPa), however this resulted in low yields and selectivities (26% yield, 20% *ee*, 1.4:1 *exo/endo*).⁷ Building on our previous studies of Diels-Alder-initiated organocascades with chiral α,β -unsaturated acylammonium salts (Figure 1, *e.g.* **2**),^{8,9} we reasoned that the termination step of a Diels-Alder-lactamization (DAL) organocascade (Figure 1, *e.g.* **3** → **7**) could provide a solution to the reversibility of these cycloadditions with furanyl dienes by careful choice of a suitable pendant, terminating nucleophile. Herein we describe the successful implementation of this strategy leading to the first highly enantioselective DA cycloadditions with a furanyl diene through a Diels-Alder lactamization cascade employing organocatalysis. Enantioselectivity and diastereoselectivity were rationalized by computational studies and applications of this methodology are presented.

We began our studies with furans bearing pendant alcohols but discovered that these gave nearly racemic cycloadducts. Presumably this is due to reversible DA cycloaddition following the initial enantioselective DAL organocascade due to a slow lactonization step or a subsequent non-enantioselective intramolecular DA cycloaddition following ester formation.^{10,11} Further evidence for a racemization pathway involving *retro*-DA followed by intramolecular DA came from monitoring the enantiopurity of cycloadducts as a function of time (see ESI, Table S1) showing a decrease in enantiopurity with prolonged reaction times.

On the other hand, use of a furan bearing a secondary pendant amine, namely furanyl *p*-tolylsulfonamide **8a**, in the DA lactamization organocascade led to greater success (Scheme 1). Employing our standard conditions developed previously for other dienes^{8,9} but employing less expensive levamisole hydrochloride (10 mol%) as Lewis base promoter, gave the *oxa*-bridged, *trans*-fused bicyclic γ -lactam **10** in 76% yield and 91% *ee* as a single *exo*-diastereomer (>19:1, ¹H NMR 500 MHz). Importantly, this bicyclic γ -lactam could be stored at ambient temperature (23 °C) for an extended period without racemization pointing to much greater stability compared to analogous lactone adducts. Thus, it appears in this case that the conversion of the cycloadducts to lactams precludes cycloreversion and racemization through intramolecular DA cycloaddition and enables a successful enantioselective, organocascade process.

To gain further insights into this cycloaddition, in particular the requirements of the pendant nucleophile, we studied various substituents with varying electronic and steric properties on the pendant amine, namely dienes **8a–i** (Table 1). For this study, we employed ethyl fumaroyl chloride (**11a**) and (*S*)-(–)-BTM as Lewis base promoter. Predictably, attempted DAL with furan **8b**, containing a sterically demanding trityl group failed, likely due to a

slow lactamization step (Table 1, entry 1). Similarly, furanyl dienes **8c–e** possessing tert-butoxycarbonyl (Boc), benzoyl (Bz), and 4,5-dibromofuranyl groups did not afford the corresponding lactams **12b–d** (Table 1, entries 2–4), likely due to the reduced nucleophilicity of these amine derivatives retarding the rate of lactamization. On the other hand, the nucleophilic benzylamine-containing furan **8f** generated the desired cycloadduct **12f** in 92% yield (Table 1, entry 5), however as a racemate, suggesting initial *N*-acylation followed by a non-enantioselective intramolecular DA cycloaddition revealing a possible non-selective background pathway for these DAL processes.

We next screened several *para*-substituted sulfonamides **8g–i** to study the electronic effects of the *N*-substituent on the lactamization step in comparison to the *N*-Ts substituted diene **8a**. The effect on enantioselectivity due to *para*-substituents of the *N*-sulfonamides was investigated and found to follow the order: NO₂ < CF₃ < Me < OMe (Table 1, entries 7–10). This trend is consistent with increasing acidity of the corresponding sulfonamides.¹² In the case of *p*-NO₂ sulfonamide furan **8g**, the greater acidity may lead to initial *N*-acylation and a competitive, racemic intramolecular DA pathway. As anticipated, in the absence of a chiral Lewis base, a substantial background DAL was found, with the *p*-NO₂ sulfonamide furan **8g** affording a single *exo*-diastereomer of racemic bicyclic γ -lactam (\pm)-**12g** albeit in modest 28% yield (Table 1, entry 6). Thus, in this series the *p*-OMe sulfonamide diene **8i** provided the best results employing 1.0 equiv of (*S*)-(-)-BTM leading to the cycloadduct **12i** in 82% ee (75% yield). However, the differential cost of tosyl chloride (TsCl ~\$0.06/g) compared to methoxy benzene sulfonyl chloride (MbsCl ~\$6/g) led us to continue optimization with furanyl *p*-toluene sulfonamide **8a**. Lowering the catalyst loading to 20 mol% delivered the bicyclic γ -lactam **12a** (Table 1, entry 11) with comparable yield (86%) but diminished enantiocontrol (42% ee). Use of pyridine, improved the enantioselectivity dramatically to 83% ee (88% yield, Table 1, entry 12) and may be due to rapid deprotonation with this base compared to the more sterically encumbered base, 2,6-lutidine, which reduces opportunity for reversible DAL. Extending the addition times of acid chloride **11** (Table 1, entry 13) by syringe pump addition led to high enantioselectivity (85% yield, 92% ee) presumably by enabling the asymmetric DAL process to compete effectively with the non-selective background pathway.

In addition to acryloyl and ethyl fumaroyl chloride, we investigated other dienophiles including crotonyl, α -methyl, and β -phenyl acryloyl chloride which, not unexpectedly, did not yield detectable amounts of cycloadduct under the optimized conditions due to the low reactivity of furanyl dienes. However, the electron deficient trifluorocrotonyl chloride **11b** participated under identical conditions to provide the corresponding fluorinated cycloadduct **13** in 54% yield and 85% ee (Scheme 2).

The possibility of a facile *retro*-DA reaction between these furan-derived cycloadducts and the isothioureia-bound α,β -unsaturated acylammonium salt in conjunction a potentially terminating lactamization step led us to study the energetics of this organocascade computationally. We optimized transition state structures (TSSs), reactants, and products for the DA step with diene **8a**, fumaroyl chloride (**11**), and (-)-(*S*)-BTM and their computed relative free energies are shown in Figure 2a. All structures were optimized with Gaussian 09¹⁶ using the M06-2X^{17,18} functional and the 6-31G(d)^{19,20} basis set. Solvent effects were

modelled using the SMD continuum model with implicit dichloromethane.²¹ The identities of TSSs were verified by the presence of one imaginary frequency and confirmed with intrinsic reaction coordinate (IRC)^{22–24} calculations.²⁵

The computed free energy barriers for the *retro*-DA cycloaddition were found to be approximately 19 – 23 kcal/mol (G), consistent with reversibility at 23 °C (Figure 2). The DA reactions were found to be concerted, but highly asynchronous, with one C–C bond formation preceding the other (e.g. TS^1_{exo} and TS^1_{endo} in Figure 2). For the *endo* pathway, a structure resembling an intermediate for a stepwise process could be optimized to a minimum (e.g. INT^1_{endo} in Figure 2), but this structure is higher in energy than the flanking TSSs (TS^1_{endo} and TS^2_{endo}) when zero-point energy corrections and/or entropy is taken into account. In other words, conversion of structures resembling intermediates in stepwise cycloaddition pathways are predicted to collapse to cycloadducts without a barrier.

Complete pathways for conversion of the cycloadducts to lactam products were not modelled due to various issues with solvent participation, proton transfers, etc.; however, lactam products were optimized to a minimum and their free energies were calculated relative to separated reactant species (Figure 3). The free energies are 2.9 and –12.4 kcal/mol for the *endo* (**10'**) and *exo* (**10**) lactams, respectively, pointing to a potentially reversible lactamization process (optimized geometries and coordinates available in the ESI) and in particular for the *endo* adduct **10'**. We expect this reversibility comes from the addition of the BTM catalyst to the lactam to reform cycloadducts followed by *retro*-DA. While the *exo* (+)-**10** lactam is thermodynamically favoured, due to reduced angle strain and the *gauche* effect, we predict the *endo* **10'** diastereomer, for which formation is endergonic, will reverse quickly to the corresponding cycloadduct, providing a relief in ring strain (Figure 2b).^{26,27} For the *exo* lactam, the nitrogen and bridged oxygen are *gauche*, which allows for a favourable $\sigma_{C-H} \leftrightarrow \sigma^*_{C-O}$ interaction. However, the N and O are *anti* in the *endo* lactam, resulting in a less favourable interaction between the σ_{N-C} orbital, a worse donor, and the σ^*_{C-O} . The reversibility of the *endo*-DA adduct could not be tested experimentally since it was never isolated, however we verified that the *exo*-adduct does not undergo reversible DA since no erosion of enantioselectivity was observed upon resubjection to the reaction conditions. Alternatively, lactamization of the *endo* cycloadduct may have too high a barrier to compete with lactamization to the *exo* lactam. This would lead to a Curtin-Hammet situation in which the *endo/exo* DA adducts can equilibrate but the differential G for the lactamization leads to exclusive formation of the *exo* adduct.

Toward demonstrating the utility of the described DAL organocascade process, we targeted further functionalization of cycloadducts and applications to the core structures of two bioactive molecules, an isatisine A derivative and a non-peptidyl grehlin-receptor inverse antagonist (Figure 4). The acetonide derivative of the natural product (–)-isatisine A was an artifact obtained during isolation found to exhibit cytotoxic activity against the leukemic C8166 cell line and also anti-HIV activity.²⁸ Lactam (+)-**12a** was converted in a three-step, single-pot process to a fully substituted tetrahydrofuran (–)-**15** with correspondence to the core structure of (–)-isatisine A. The process involved ozonolytic cleavage of the olefin followed by *in situ* double Wittig olefination to deliver diester (–)-**15**. The cycloadduct **12a**, bearing an *oxa*-bridged tricyclic γ -lactam, also bears resemblance to the nonpeptidyl

ghrelin-receptor inverse agonists that were recently disclosed by 7TM Pharma.²⁹ In addition, epoxidation of the tricyclic γ -lactam (+)-**12a** furnished a fully substituted cyclohexane bearing four fused rings with six contiguous stereogenic centers, (+)-**14**, as needle-like crystals. This enabled unambiguous assignment of the absolute and relative configuration of cycloadduct (+)-**12a** (Figure 4, inset; ESI, Figure S1).

In summary, the first highly enantio- and diastereoselective organocatalytic DA cycloaddition of a furanyl diene is described through a Diels-Alder-lactamization organocascade employing chiral, α,β -unsaturated acylammonium salts as dienophiles. The use of a furan with a pendant sulfonamide led to the generation of *oxa*-bridged *trans*-fused tricyclic γ -lactams. Computational evidence was gathered to support the notion that these DAL organocascades are susceptible to thermodynamic control through potential reversible lactamization and Diels-Alder steps. While the scope of this furan DAL is limited at this time to highly electron-poor dienophiles, the striking simplicity, excellent diastereo- and enantioselectivity, and high yields obtained with commodity acid chlorides including acryloyl and fumaroyl chloride render this a promising process for *de novo*, rapid synthesis of polycyclic scaffolds including heterocyclic rings with multiple stereocenters useful for diversity-oriented synthesis.

Supplementary Material

Refer to Web version on PubMed Central for supplementary material.

Acknowledgments

Support from NSF (CHE-1112397 to D.R.; CHE-030089 with XSEDE to D.J.T.), the Robert A. Welch Foundation (AA-1280 to D.R.), ACS PRF (52801-ND4 to D.J.T.), and partial support from NIH (GM 052964 to D.R.) is gratefully acknowledged. Drs. Nattamai Bhuvanesh and Joe Reibenspies (Center for X-ray Analysis, TAMU) secured X-ray data, and Dr. Bill Russell (Laboratory for Biological Mass Spectrometry, TAMU) provided mass data.

References

1. Tobia D, Harrison R, Phillips B, White TL, DiMare M, Rickborn B. *J Org Chem.* 1993; 58:6701. Foster RW, Benhamou L, Porter MJ, Bu ar DK, Hailes HC, Tame CJ, Sheppard TD. *Chemistry.* 2015; 21:6107. [PubMed: 25756502]
2. Warren RN, Margetic D, Sun G. *Tetrahedron Lett.* 2001; 42:4263. Zubkov FI, Zaytsev VP, Nikitina EV, Khrustalev VN, Gozun SV, Boltukhina EV, Varlamov AV. *Tetrahedron.* 2011; 67:9148. Froidevaux V, Borne M, Laborbe E, Auvergne R, Gandini A, Boutevin B. *RSC Adv.* 2015; 5:37742. Lacerda TM, Carvalhoc AJF, Gandini A. *RSC Adv.* 2016; 6:45696.
3. Evans DA, Barnes DM. *Tetrahedron Lett.* 1997; 38:57.
4. Evans DA, Barnes DM, Johnson JS, Lectka T, von Matt P, Miller SJ, Murry JA, Norcross RD, Shaughnessy EA, Campos KR. *J Am Chem Soc.* 1999; 121:7582.
5. Ryu DH, Kim KH, Sim JY, Corey EJ. *Tetrahedron Lett.* 2007; 48:5735.
6. Liu D, Canales E, Corey EJ. *J Am Chem Soc.* 2007; 129:1498. [PubMed: 17283985]
7. Mimoto A, Nakano K, Ichikawa Y, Kotsuki H. *Heterocycles.* 2010; 80:799.
8. Abbasov ME, Hudson BM, Tantillo DJ, Romo D. *J Am Chem Soc.* 2014; 136:4492. [PubMed: 24588428] Abbasov ME, Hudson BM, Tantillo DJ, Romo D. *Chem Sci.* 2017; 18:1511.
9. Bappert E, Muller P, Fu GC. *Chem Commun.* 2006; 2604. Pandiancherri S, Ryan SJ, Lupton DW. *Org Biomol Chem.* 2012; 10:7903. [PubMed: 22930129] Robinson ERT, Fallan C, Simal C, Slawin AMZ, Smith AD. *Chem Sci.* 2013; 4:2193. Liu G, Shirley ME, Van KN, McFarlin RL, Romo D. *Nat*

- Chem. 2013; 5:1049. [PubMed: 24256870] Vellalath S, Van KN, Romo D. *Angew Chem, Int Ed.* 2013; 52:13688. Fukata Y, Okamura T, Asano K, Matsubara S. *Org Lett.* 2014; 16:2184. [PubMed: 24684317] Fukata Y, Asano K, Matsubara S. *J Am Chem Soc.* 2015; 137:5320. [PubMed: 25856510] Matviitsuk A, Taylor JE, Cordes DB, Slawin AM, Smith AD. *Chemistry-A European Journal.* 2016; 22:17748. Robinson ER, Frost AB, Elías-Rodríguez P, Smith AD. *Synthesis.* 2017; 49:409.; For a recent review on unsaturated acylammonium salts, see: Vellalath S, Romo D. *Angew Chem, Int Ed.* 2016; 55:13934.. For a potentially related organocascade involving acyl cyanides, see: Gouedranche S, Bugaut X, Constantieux T, Bonne D, Rodriguez J. *Chem Eur J.* 2014; 20:410. [PubMed: 24307550]
10. Jung ME, Gervay J. *Tetrahedron Lett.* 1988; 29:2429.
 11. Jung ME, Gervay J. *J Am Chem Soc.* 1989; 111:5469.
 12. anli S, Altun Y, anli N, Alsancak G, Beltran JL. *J Chem Eng Data.* 2009; 54:3014.
 13. Steinreiber J, Faber K, Griengl H. *Chem Eur J.* 2008; 14:8060. [PubMed: 18512868]
 14. Córdova A, Ibrahim I, Casas J, Sundén H, Engqvist M, Reyes E. *Chem Eur J.* 2005; 11:4772. [PubMed: 15929141]
 15. Steinreiber J, Schürmann M, Wolberg M, van Assema F, Reisinger C, Fesko K, Mink D, Griengl H. *Angew Chem Int Ed.* 2007; 46:1624.
 16. Frisch, MJ., et al. *Gaussian 09, Revision D.01.* Gaussian, Inc; Wallingford CT: 2009.
 17. Zhao Y, Truhlar D. *Theor Chem Acc.* 2008; 120:215.
 18. Zhao Y, Truhlar DG. *Acc Chem Res.* 2008; 41:157. [PubMed: 18186612]
 19. Petersson GA, Bennett A, Tensfeldt TG, Allaham MA, Shirley WA, Mantzaris J. *J Chem Phys.* 1988; 89:2193.
 20. Petersson GA, Allaham MA. *J Chem Phys.* 1991; 94:6081.
 21. Marenich AV, Cramer CJ, Truhlar DG. *J Phys Chem B.* 2009; 113:6378. [PubMed: 19366259]
 22. Fukui K. *Acc Chem Res.* 1981; 14:363.
 23. Gonzalez C, Schlegel HB. *J Phys Chem.* 1990; 94:5523.
 24. Maeda S, Harabuchi Y, Ono Y, Taketsugu T, Morokuma K. *Int J Quant Chem.* 2015; 115:258.
 25. Ball-and-stick images of computed structures were created with CYLview, 1.0b. Legault, C. Y: Université de Sherbrooke; 2009. (<http://www.cylview.org>)
 26. Alabugin, IV., editor. *Stereoelectronic Effects: A Bridge Between Structure and Reactivity.* 1. John Wiley & Sons Ltd; 2016.
 27. Black KA, Wilsey S, Houk KN. *J Am Chem Soc.* 2003; 125:6715. [PubMed: 12769581]
 28. Liu JF, Jiang ZY, Wang RR, Zheng YT, Chen JJ, Zhang XM, Ma YB. *Org Lett.* 2007; 9:4127. [PubMed: 17850153]
 29. Linnanen, T., Rist, O., Grimstrup, M., Frimurer, T., Hoegberg, T., Nielsen, FE., Gerlach, LO. *WO* 2008/092681. 2008.

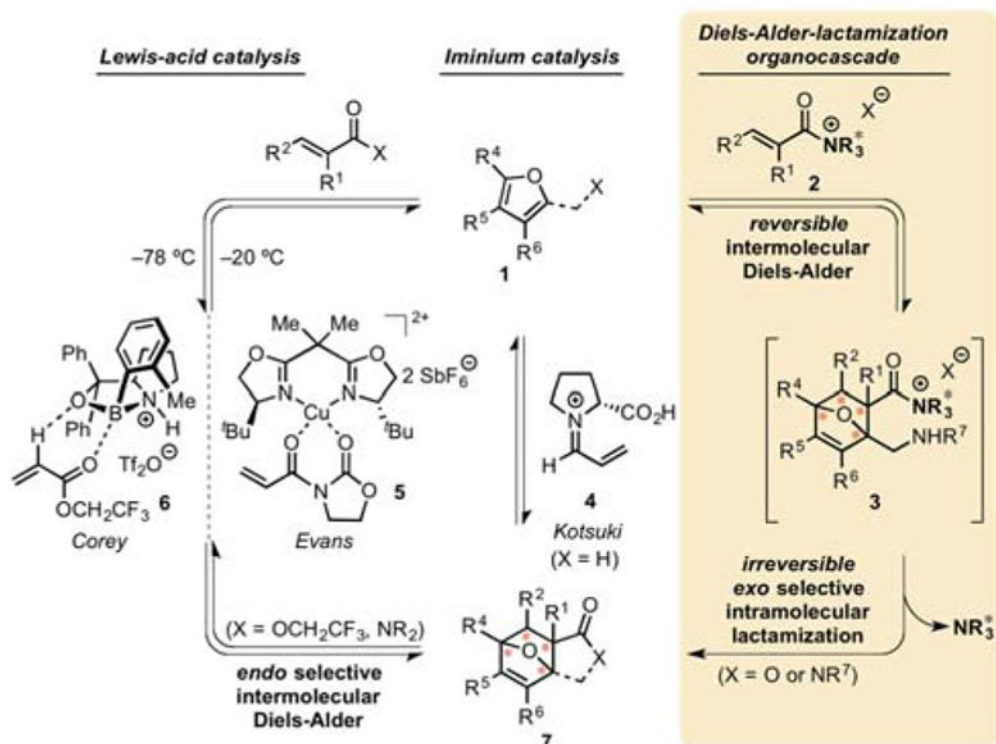


Figure 1. Comparison of enantioselective Diels-Alder cycloadditions with furans as dienes. Lewis-acid catalyzed, iminium-based, and the current asymmetric, α,β -unsaturated acylammonium salt-based, Diels-Alder-lactamization organocascade.

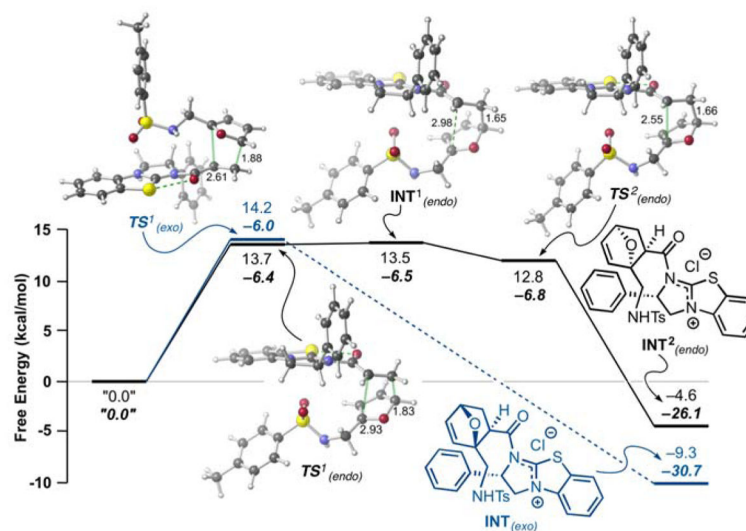


Figure 2. Calculated TSSs for the DA step (optimized with SMD(DCM)-M06-2X/6-31G(d)). Free energies (G, normal text) and enthalpies (H, bold, italic) are shown relative to separated reactant species, furan **8a**, acryloyl chloride (**9**), and (*S*)-(-)-BTM (energies in kcal/mol).

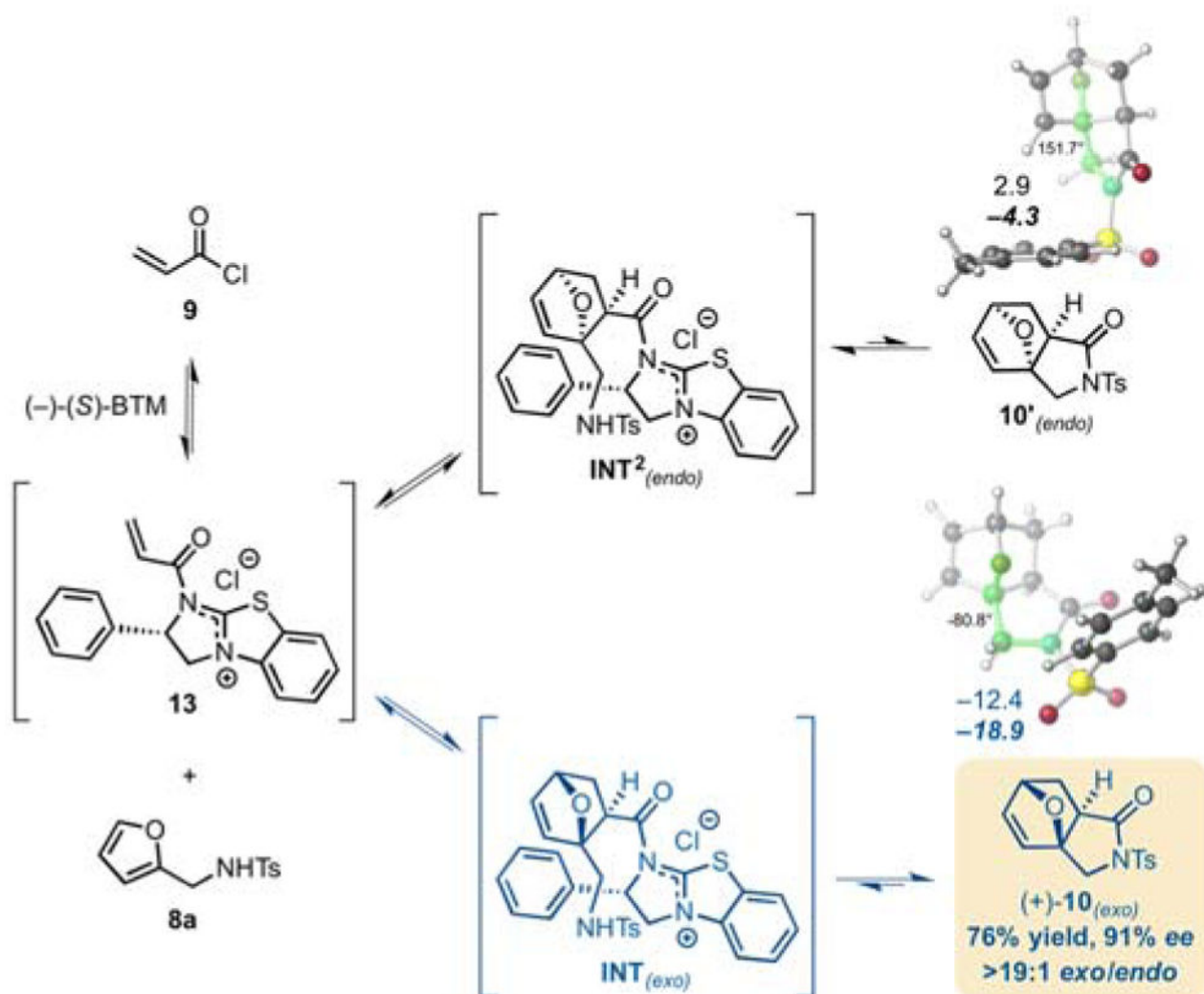
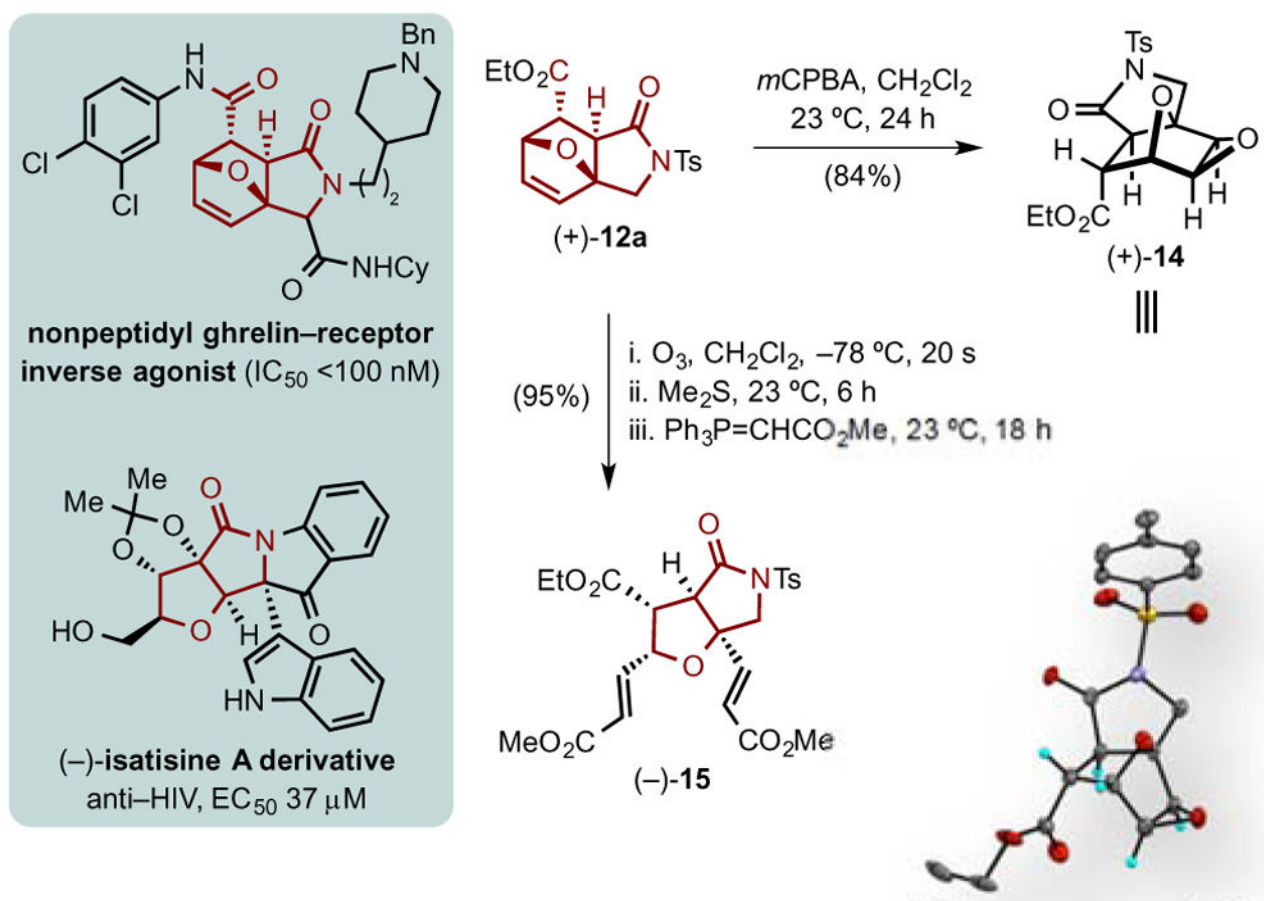
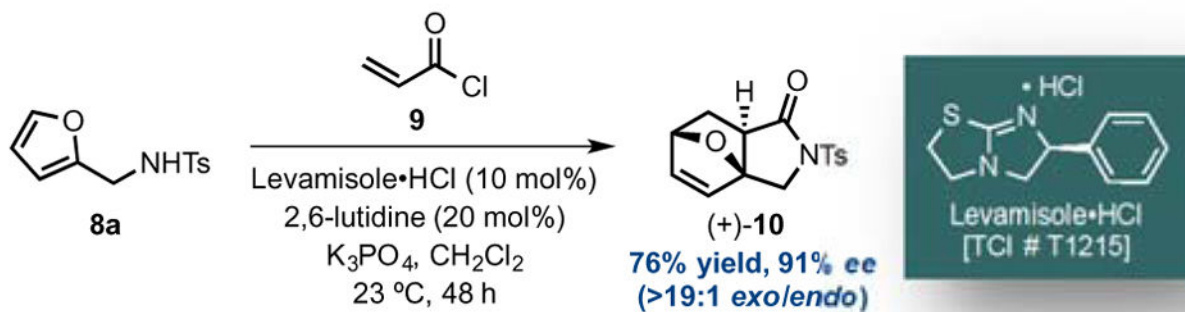


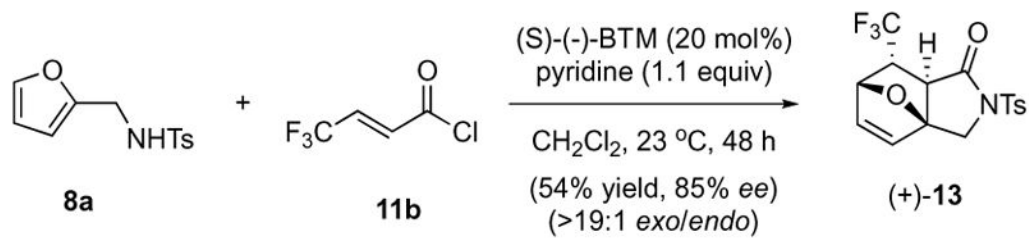
Figure 3. Potential funneling of *endo* **10'** diastereomer to the thermodynamically favored *exo* **(+)-10** diastereomer involving a *retro*-Diels-Alder/Diels-Alder-lactamization sequence. Optimized geometries of *endo* **10'** and *exo* **(+)-10** lactams calculated using SMD(DCM)-M06-2X/6-31G(d). Select dihedral angles (O-C-C-N, green) are shown.

**Figure 4.**

Epoxidation of tricyclic γ -lactam (+)-**12a** to a fully substituted *oxa*-bridged cyclohexane (+)-**14** with six contiguous stereocenters. Transformation of (+)-**12a** to a fully substituted tetrahydrofuran (-)-**15** with correspondence to the natural product, isatisine A. (Inset: single crystal X-ray structure in ORTEP format of (+)-**14**; 50% probability, see ESI Figure S1).

**Scheme 1.**

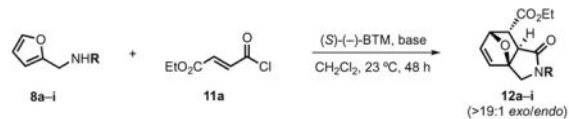
Diels-Alder-lactamization of furan-based sulfonamide **8a** and acryloyl chloride (**9**) mediated by (*R*)-(-)-levamisole hydrochloride providing bridged cycloadduct (+)-**10**.

**Scheme 2.**

Diels-Alder-lactamization of furan **8a** and trifluorocrotonyl chloride (**11b**) delivering bridged cycloadduct (+)-**13**.

Table 1

Varying the *N*-substituent on amino furans **8** for the enantioselective DAL organocascade with acid chloride **11a** providing lactams **12**.^a



entry	cycloadducts R(12)	catalyst loading (mol%)	base	ee (yield [†]) %
1	CPh ₃ (12b)	100	2,6-lutidine	<i>n.r.</i>
2	Boc (12c)	100	2,6-lutidine	<i>n.r.</i>
3	Bz (12d)	100	2,6-lutidine	<i>n.r.</i>
4	 (12e)	100	2,6-lutidine	<i>n.r.</i>
5	Bn (12f)	100	2,6-lutidine	3 (92)
6	 (12g)	0	2,6-lutidine	-(28)
7	 (12h)	100	2,6-lutidine	40 (46)
8	 (12h)	100	2,6-lutidine	51 (40)
9	 (Ts, 12a)	100	2,6-lutidine	70 (75)
10	 (12i)	100	2,6-lutidine	75 (82)
11	Ts	20	2,6-lutidine	42 (86)
12	Ts	20	pyridine	83 (88)
13 [‡]	Ts	20	pyridine	94 (85)

^aDAL reactions were performed with dienes **8** (1.0 equiv), ethyl fumaroyl chloride (**11a**, 1.2 equiv), (*S*)-(-)-BTM (20–100 mol%) and Brønsted base (1.0 equiv) in CH₂Cl₂ (0.1 *M*).

[†]All yields refer to isolated, purified yields of cycloadducts. Diastereomeric (*endo/exo*) ratios were determined by ¹H NMR (500 MHz) analysis of the crude reaction mixtures. Enantiomeric excess (*ee*) was determined by chiral phase HPLC.

[†]Fumaroyl chloride **11a** was added as a solution in CH₂Cl₂ by syringe pump over 5 h.

Author Manuscript

Author Manuscript

Author Manuscript

Author Manuscript